Van der Waals bond lengths and electronic spectral shifts of the benzene–Kr and benzene–Xe complexes

Th. Weber, E. Riedle [1], H.J. Neusser and E.W. Schlag
Institut für Physikalische und Theoretische Chemie, Technische Universität München, Lichtenbergstrasse 4, W-8046 Garching, Germany

Received 13 May 1991; in final form 10 June 1991

Rotationally resolved UV-spectra are presented for the 6_0^1 bands of benzene–Kr and benzene–Xe complexes yielding precise rotational constants and van der Waals bond lengths for the ground and excited vibronic state, and electronic band shifts. These values complement the previously published data for the other rare gases and the various quantities have now been determined for all the benzene–rare gas complexes. Measured values of the bond length were used to calculate the band shifts from recent theoretical predictions. They are compared with the experimental values of this work.

1. Introduction

The goal of this work is to obtain a complete set of exact structural data for all the benzene–rare gas (1:1) complexes (C_6H_6–R). In particular, we wish here to complete this homologous series by results for Kr and Xe.

Benzene–rare gas clusters are prototype systems for weakly bound van der Waals clusters between two nonpolar elements. Due to a nonexisting dipole moment in benzene on the one hand, and the isotropic atomic charge distribution on the other hand, the intermolecular interaction potential is dominated by dispersion forces. Thus, benzene–rare gas clusters are ideal systems to study this type of interaction. Furthermore, the high symmetry of benzene suggests a simple structure of C_6H_6–R with the noble gas atom located on the sixfold rotational axis of benzene. For these reasons, individual C_6H_6–R complexes have been studied both theoretically [1–6] and experimentally [7–14], during the last decade.

The most accurate data on the structure of these complexes have emerged from rotationally resolved spectroscopy. In the early work of Beck et al. [7], the relatively low spectral resolution of 1.3 GHz still yielded a few well-resolved rovibronic lines in the UV-spectrum of the 6_0^1 band in benzene–He thanks to the very efficient cooling ($T_{rot} \approx 0.3$ K) in a continuous supersonic jet. Improving an earlier low-resolution study of the vibronic band structure of Fung et al. [15], we recently succeeded in resolving more than 200 lines of the 6_0^1 band of benzene–Ar at a higher rotational temperature of 2–4 K [12]. This was feasible because of the high spectral resolution of 130 MHz of a pulsed amplified cw laser source and a mass-selective detection of $(benzene\text{–}Ar)^+$ ions after two-color resonance-enhanced two-photon ionization.

Both experiments on benzene–He and benzene–Ar clearly demonstrate that the noble gas atom is indeed located on the sixfold symmetry axis of benzene. Its averaged van der Waals distance from the benzene plane in the S_0 (S_1) state was determined to be 3.17 ± 0.37 (3.25 ± 0.26) Å for benzene–He and, with a higher accuracy, to be 3.581 ± 0.001 (3.521 ± 0.002) Å for benzene–Ar. Very recently, for the benzene–Ar complex, ground-state rotational constants with improved accuracy became available from microwave spectroscopy [16], which, in addition, confirmed the values determined from high-resolution UV-spectroscopy. In recent work, as a fur-

[1] Present address: Joint Institute for Laboratory Astrophysics, University of Colorado and National Institute of Standards and Technology, Boulder, CO 80309-0440, USA (1991–1992 visiting fellow).

ther example, we presented the rotationally resolved UV-spectra of two isotopic benzene–Ne clusters (C_6H_6–^{20}Ne and C_6H_6–^{22}He) and their van der Waals bond distances [13].

In this work, rotationally resolved spectra of the two remaining C_6H_6–R complexes, i.e. benzene–Kr and benzene–Xe, are presented. The experimental data – van der Waals bond lengths and spectral band shifts – for different noble gas atoms will be discussed in terms of their different polarizabilities.

2. Experimental

Mass-selected vibronic spectra of benzene–Kr and benzene–Xe were recorded by resonance-enhanced two-color two-photon ionization in a time-of-flight (TOF) mass-spectrometer as described in our previous papers [12,13,17–19]. The species-dependent conditions of the cluster formation are to be discussed in more detail below.

The clusters were produced in a supersonic jet expansion [20] of a premixed gas sample. For the measurements of benzene–Kr, a mixture of 6 mbar benzene and 5 bar Kr was employed. This mixture yielded a signal-to-noise ratio and a rotational cooling comparable to that of the benzene–Ar spectra. For benzene–Xe, neither a pure mixture of benzene and Xe (6% benzene in 600 mbar Xe) nor a mixture with additional 5 bar He yielded a satisfactory cluster formation. Finally, a gas sample of 40 mbar benzene, 560 mbar Xe, and 4 bar Kr was mixed and kept for 20 h for improved mixing of the different components. This gave a reasonable sample for rotationally resolved measurements, although the ion signal was still quite small. Thus, the maximum available energy of both laser pulses had to be used (excitation: 1 mJ/cm^2; ionization: 20 mJ/cm^2 at 2700.0 Å) to achieve a satisfactory signal-to-noise ratio. The high laser intensity caused some line broadening in the spectrum of benzene–Xe (see below).

3. Results

3.1. Benzene–Kr

Kr exists in several stable isotopic modifications, ^{78}Kr, ^{80}Kr, ^{82}Kr, ^{83}Kr, ^{84}Kr, and ^{86}Kr, with a natural abundance of 0.4%, 2.2%, 11.6%, 11.5%, 57.0%, and 17.3%, respectively. The two isotopic van der Waals clusters C_6H_6–^{84}Kr and C_6H_6–^{86}Kr were investigated individually from their natural isotopic mixture. This was feasible due to the mass selectivity of the ion-detection technique used in this work.

In fig. 1, the rotationally resolved spectra of the strongest vibronic band, the 6_0^1 band at 38573 cm^{-1}, are shown for both isotopes. The upper (lower) spectrum was obtained when ions with 164 au (162 au) were monitored. The vertical scale of the upper spectrum is increased by a factor of 3 to compensate for the smaller abundance of ^{86}Kr and the resulting smaller ion signal. Both bands display the rotational structure of a prolate symmetric top similar to that of the same band in benzene–Ar [12]. Briefly, the resolved strong lines on the low- and high-energy side of the band are from the P- and R-branch, respectively. Their linewidth is $\approx$150 MHz (fwhm) and represents the experimental resolution given by the convolution of the frequency width of the UV laser pulse (130 MHz) and the remaining Doppler width of the skimmed beam (50 MHz). The seven strong broad features in the center of the band are subbranches of the Q-branch with partially overlapping rotational lines. The blue-shaded wings of the subbands originate from lines with constant K' and ΔK but varying J'. As in benzene–Ar, the blue-shading indicates an increased B rotational constant in the S_1 state of the cluster.

The differences in structure of the two isotopic bands and in the line positions cannot be recognized by naked eye, but only in the detailed analysis of the data. This is due to the small relative mass change of the two isotopic clusters of only 1.2%.

For a precise determination of the rotational constants of the bands, a computer fit to the line positions was performed, according to the procedure described in detail in our recent work [13]. After selection of rotational transitions in the spectrum leading to the same excited rotational state but originating from different ground rotational states ("combination differences"), we were able to determine the ground-state rotational constant B_0'' with high accuracy. The centrifugal distortion constants could not be determined at the present spectral resolution and with observation of only low J-value

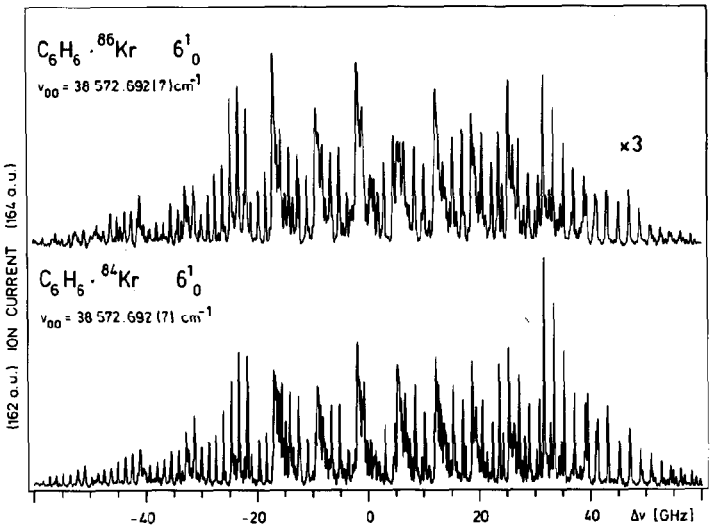

Fig. 1. Mass-selected rotationally resolved spectrum of the 6^1_0 band of C_6H_6–^{86}Kr (upper trace) and C_6H_6–^{84}Kr (lower trace) measured in natural isotopic abundance. Note the increased vertical scale of the less-abundant C_6H_6–^{86}Kr isotopic cluster.

transitions, and were, therefore, constrained to zero. In a second step, the rotational constants A'_v, B'_v and the Coriolis coupling constant ζ'_{eff} of the excited 6^1 state and the band origin ν_{00} were fitted using 150 (75) unblended rotational lines of the experimental spectrum of C_6H_6–^{84}Kr (C_6H_6–^{86}Kr). Here, it was assumed that the rotational constant A''_0 is identical with the rotational constant C''_0 in benzene, i.e. the bond lengths in benzene are not changed in the cluster.

The rotational constants obtained from the fit are listed in table 1. For comparison, the experimental values for all C_6H_6–R complexes are given. The less-accurate values for benzene–He were taken from the work of Beck et al. [7], the other values are from measurements of our group.

From the rotational constants and the symmetric-top structure, accurate values of the bond distance of Kr from the benzene plane were calculated, as listed in table 1. It should be noted that a decrease of the van der Waals bond length upon electronic excitation is observed, as was seen for Ne [13] and Ar [12].

3.2. Benzene–Xe

In the natural mixture, ^{129}Xe, ^{131}Xe, and ^{132}Xe are present with an abundance of 26.4%, 21.2%, and 26.9%, respectively. The mass resolution of the TOF mass-spectrometer ($m/\Delta m \approx 300$, fwhm) was not sufficient to separate completely the mass peaks of C_6H_6–^{131}Xe (209 au) and C_6H_6–^{132}Xe (210 au). Thus, the individual spectra measured for these ion masses contain contributions from the neighbouring mass. This problem does not exist for C_6H_6–^{129}Xe. Therefore, we present the spectrum of the 6^1_0 band of this isotopic cluster (see fig. 2). The quality of the spectrum is lower than that of the benzene–Kr spectrum shown in fig. 1, due to a lower signal-to-noise ratio and a lower effective resolution leading to a linewidth of more than 400 MHz. The ultimate reason for both effects is the low concentration of benzene–Xe clusters in the supersonic beam which in turn required a higher intensity of both laser beams to observe a measurable ion signal. The high intensity of the first laser pulse leads to a saturation and broadening of the first transition to the 6^1 state, and the high intensity of the second laser pulse shortens the effective lifetime of the 6^1 state by a high absorption rate of the ionizing step. Despite the lower quality of the spectrum, the three rotational branches are still identifiable. The rotational structure is very similar to that of benzene–Ar_2 [19] and indeed the rotational constants of both clusters are found to be very similar.

Table 1
Spectroscopic constants and averaged van der Waals bond lengths derived from the analysis of the rotationally resolved spectra of the 6_0^1 band of all benzene–noble gas clusters. ν_{00} is the absolute frequency of the band origin in cm^{-1}. $A(C)$ and B are the symmetric-top rotational constants in cm^{-1}. ζ_{eff} is the effective Coriolis coupling constant for the excited degenerate vibronic state. $\langle r \rangle$ is the vibrationally averaged distance of the noble gas atom from the center-of-mass of benzene in Å derived from the B rotational constant. Symbols with " and ' refer to the ground and electronically excited state, respectively. N is the number of assigned unblended rovibronic lines and σ the standard deviation of the fit in MHz

	R						
	^4He [a]	^{20}Ne [b]	^{22}Ne [b]	^{40}Ar [c]	^{84}Kr [d]	^{86}Kr [d]	^{129}Xe [d]
ν_{00}	38608.39(3)	38603.223(8)	38603.215(8)	38585.071(8)	38572.692(7)	38572.692(7)	38552.423(12)
$A_0''(C_0'')$		0.0948809	0.0948809	0.0948809	0.0948809	0.0948809	0.0948809
$A_v'(C_v')$		0.090779(8)	0.090798(14)	0.090866(3)	0.090838(5)	0.090839(15)	0.09096(16)
B_0''	0.130(10)	0.060341(11)	0.057424(14)	0.039402576(4)	0.026562(13)	0.026263(21)	0.02118(20)
B_v'	0.124(7)	0.060448(11)	0.057563(14)	0.040090(2)	0.027266(15)	0.026962(24)	0.02187(22)
$B_v'-B_0''$	−0.006(17)	+0.000107(2)	+0.000139(2)	+0.000687(2).	+0.000704(1)	+0.000699(2)	+0.000690(2)
ζ_{eff}'	−0.57(5)	−0.5909(3)	−0.5907(4)	−0.5869(9)	−0.5858(1)	−0.5862(3)	−0.584(4)
$\langle r'' \rangle$	3.17(37)	3.460(1)	3.454(1)	3.581(1)	3.674(2)	3.677(2)	3.814(20)
$\langle r' \rangle$	3.25(26)	3.420(3)	3.415(3)	3.521(2)	3.605(2)	3.608(3)	3.735(22)
N	9	74	67	226	150	75	28
σ		18.4	23.0	29.6	23.2	22.7	76.4

[a] Taken from ref. [7].
[b] Taken from our recent work [13].
[c] The values differ slightly from the ones published in our recent work [12]. They are calculated with the very precise values for the B_0'', D_J'' and D_{JK}'' rotational constants recently measured by microwave spectroscopy [16] and the additional assumptions $D_K''=0$ and $\Delta D=0$.
[d] This work.

The rotational constants of C_6H_6–^{129}Xe were determined by a global fit to 28 selected and identified rotational lines. An application of the "combination differences" method was not possible due to the small number of unblended lines.

The rotational constants as well as the calculated van der Waals bond lengths are given in table 1. Again, the bond length is decreased upon electronic excitation.

4. Discussion

The rotational analysis described above yields precise values for the positions of the 6_0^1 band origin, i.e. the pure vibronic transition frequencies of the benzene–Kr and benzene–Xe clusters. From these results and the precise position of the 6_0^1 band origin in the benzene molecule (38606.089 cm^{-1} [20]), accurate values for the band shift in the C_6H_6–R complexes are obtained. They are summarized in table 2. The value for benzene–He is taken from the work of Beck et al. [7]. The measured values for the band shifts in benzene–Ar and benzene–Ne are taken from our previous work [12,13].

In fig. 3, the measured band shifts are plotted as a function of the rare gas polarizability [21]. The accuracy of the experimental band shifts ($< \pm 0.02$ cm^{-1}) is much better than the size of the symbols and is, thus, not indicated in fig. 3. Approximately, a linear dependence of the measured band shift on the polarizability of the rare gas atoms Ne, Ar, Kr, and Xe is found and indicated by the solid line in fig. 3. This linear increase of the red-shift with increasing polarizability supports the conjecture, that the attractive forces of the van der Waals interaction in aromatic molecule–rare gas complexes are mainly of dispersive nature [22].

The first theoretical treatment of electronic band shifts dominated by dispersion forces was carried out

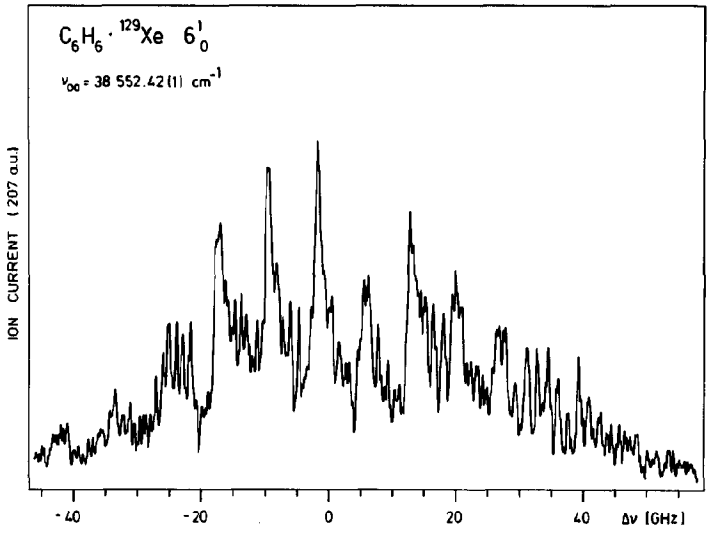

Fig. 2. Mass-selected partially rotationally resolved spectrum of the 6^1_0 band of C_6H_6–^{129}Xe. For explanation of the broader linewidth of more than 400 MHz, see text.

Table 2
Comparison of measured and calculated spectral shifts between the 6^1_0 band of benzene and the 6^1_0 band of the benzene–rare gas clusters. $\delta\nu_{00}$ is the shift of the band origin with respect to the benzene monomer in cm^{-1} (negative values indicate a red-shift of the cluster band). For explanation of the theoretical values, see text

	R				
	^{4}He	^{20}He	^{40}Ar	^{84}Kr	^{129}Xe
experimental					
$\delta\nu_{00}$	+2.30(2) [a]	−2.866(16) [b]	−21.018(16) [c]	−33.397(15) [d]	−53.666(20) [d]
calculated					
$\delta\nu_{00}$ (ref. [2])	−2.5	−7.3	−18.2	−24.6	−31.4
$\delta\nu_{00}$ [e]	−2.5	−3.9	−15.1	−20.4	−27.9
$\delta\nu_{00}$ (ref. [4])		−5.89	−29.26	−46.53	−64.28

[a] Taken from ref. [7].
[b] Taken from our previous work [13].
[c] Taken from our previous work [12].
[d] This work.
[e] Calculated from eq. (1) using the experimental bond lengths of table 1 (for details, see text).

by Longuet-Higgins and Pople [23]. They presented the following expression for the red-shift $\delta\nu_{\text{disp}}$ of electronic transitions of nonpolar molecules (M) soluted in nonpolar solvents (S):

$$\delta\nu_{\text{disp}} = \tfrac{1}{3} r^{-6} \frac{\bar{E}\bar{F}}{\bar{E}+\bar{F}-E_i} \alpha_S \times \left(\frac{E_i}{2(\bar{E}+\bar{F})} \alpha_M + \frac{|R_{0\to i}|^2}{\bar{F}-E_i} \right). \quad (1)$$

Here, r is the van der Waals distance between M and S, $\bar{E}$ and $\bar{F}$ are averaged excitation energies of M and

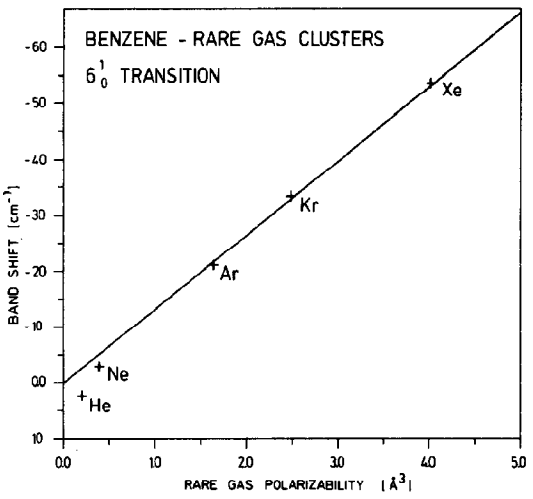

Fig. 3. Spectral shift of the 6_0^1 band, $\delta\nu_{00}$, as a function of the rare gas polarizability of the measured benzene–rare gas complexes. The polarizabilities are taken from ref. [21].

S, respectively, E_i is the electronic transition energy in M, $R_{0\to i}$ the corresponding electronic transition moment, and α_M and α_S are the ground-state polarizabilities of M and S, respectively. Although eq. (1) was evaluated for a pure electronic transition, it is also applicable to the 6_0^1 transition, since the in-plane mode ν_6 is not expected to influence the band shift [2], thus allowing the use of the measured vibronic band shifts as electronic band shifts.

Three calculations of the electronic band shift of C_6H_6–R are considered:

(i) In the recent work of Leutwyler [2], the parameters $\bar{E}$ and $\bar{F}$ were approximated by the ionization potentials of M and S. In addition, van der Waals bond lengths were calculated from the minima of empirical potentials. With these approximations, the formula in eq. (1) was used to calculate the red-shifts. In table 2, the theoretical predictions of Leutwyler [2] are compared with the measured band shifts of this work.

(ii) Rotationally resolved spectroscopy enables us to present for the first time precise experimental values for the effective van der Waals bond lengths $\langle r \rangle$ of the complete set of C_6H_6–R clusters. As can be seen from table 1, a slight reduction of the bond lengths in the S_1 state with respect to the S_0 state for all clusters, except benzene–He, is found. Thus, the assumption of a constant bond length in eq. (1) is no longer required. The influence of the change of $\langle r \rangle$ on eq. (1) was estimated by Yamanouchi et al. [24], which they found to be less than 10% of the total red-shift. Due to the smallness of this effect it is neglected in the following discussion. With our experimental values for $\langle r \rangle$, we recalculated the band shifts for the different noble gases according to eq. (1) using for the other parameters the values of ref. [2]. The results are listed in table 2.

(iii) In addition, the evaluated red-shifts of Kim and Cole [4] using calculated empirical potentials for the S_0 and S_1 state are shown for comparison.

None of the theoretical modellings conforms to our new data. The authors of ref. [4] attributed a remaining disagreement between their theoretical and the experimental data to the omission of the change in overlap repulsive energy. A likely reason for the smaller values for the red-shift in calculations (i) and (ii) is that the band shift is not solely determined by the attractive part of the potential that is taken into account in eq. (1). Near the minimum, both the repulsive and the attractive dispersive parts contribute to the van der Waals potential. The importance of the repulsive part for the electronic band shift is demonstrated by the experimental result for benzene–He [7]. Here, contrary to the red-shift in complexes of benzene with larger noble gases, a blue-shift is observed that cannot be explained by an attractive dispersive interaction alone, and, thus, must contain contributions from the repulsive part of the potential. It is concluded that the relative importance of the attractive and the repulsive interaction differs for different noble gases.

5. Summary and conclusion

In this work, rotationally resolved spectra of the 6_0^1 band of benzene–Kr and, with partial rotational resolution, for benzene–Xe are presented. The rotational analysis of the spectra yields precise rotational constants and accurate van der Waals bond lengths for the S_1 as well as for the S_0 electronic state. With these results and our previous findings for benzene–Ne [13] and benzene–Ar [12], we are now able to present a complete picture of the van der Waals bond-length change for the prototype system ben-

zene–noble gas with increasing polarizability for all different noble gas atoms.

The measured red-shifts of the 6_0^1 band clearly demonstrate that dispersion forces are the dominating contribution to the attractive van der Waals interaction. The red-shift of the band origin increases almost linearly with increasing polarizability. The measured electronic shifts are compared with recent theoretical predictions which consider dispersive attractive forces but neglect the repulsive part of the potential. Though the precise van der Waals bond lengths reported here are used in this calculation, the agreement of calculated and measured electronic band shifts is still poor. From these results, we conclude that changes in the repulsive part of the van der Waals potential have to be considered for the different noble gases, in addition to the attractive dispersion part, in order to understand the observed electronic red-shifts.

Acknowledgement

The authors thank R. Sussmann for assistance during the assignment of the spectra and Dr. A.M. Smith for careful reading of the manuscript and valuable discussions. Financial support from the Deutsche Forschungsgemeinschaft and from the Fonds der Chemischen Industrie is gratefully acknowledged.

Note added

After completion this work we learned that recent values for the B_0'' rotational constant of benzene–Kr have been found by Emilsson, Klots and Gutowsky from FT-microwave spectroscopy: 0.02654110 and 0.02628642 cm^{-1} for C_6H_6–^{84}Kr and C_6H_6–^{86}Kr, respectively [25]. They agree with the values of this work, found from the rotational analysis of an electronic spectrum.

References

[1] J. Jortner, U. Even, S. Leutwyler and Z. Berkovitch-Yellin, J. Chem. Phys. 78 (1983) 309.
[2] S. Leutwyler, Chem. Phys. Letters 107 (1984) 284.
[3] W.E. Henke, W. Yu, H.L. Selzle, E.W. Schlag, D. Wutz and S.H. Lin, Chem. Phys. 97 (1985) 205.
[4] H.-Y. Kim and M.W. Cole, J. Chem. Phys. 90 (1989) 6055.
[5] A.T. Amos, T.F. Palmer, A. Walters and B.L. Burrows, Chem. Phys. Letters 172 (1990) 503.
[6] P. Hobza, H.L. Selzle and E.W. Schlag, J. Chem. Phys., submitted for publication.
[7] S.M. Beck, M.G. Liverman, D.L. Monts and R.E. Smalley, J. Chem. Phys. 70 (1979) 232.
[8] K.H. Fung, W.E. Henke, T.R. Hays, H.L. Selzle and E.W. Schlag, J. Phys. Chem. 85 (1981) 3560.
[9] N. Gonohe, N. Suzuki, H. Abe, N. Mikami and M. Ito, Chem. Phys. Letters 94 (1983) 549.
[10] T.A. Stephenson and S.A. Rice, J. Chem. Phys. 81 (1984) 1083.
[11] J.A. Menapace and E.R. Bernstein, J. Phys. Chem. 91 (1987) 2533.
[12] Th. Weber, A. von Bargen, E. Riedle and H.J. Neusser, J. Chem. Phys. 92 (1990) 90.
[13] Th. Weber, E. Riedle, H.J. Neusser and E.W. Schlag, J. Mol. Struct., in press.
[14] M. Schmidt, M. Mons and J. Le Calvé, Chem. Phys. Letters 177 (1991) 371.
[15] K.H. Fung, H.L. Selzle and E.W. Schlag, Z. Naturforsch. 36a (1981) 1338.
[16] Th. Brupbacher and A. Bauder, Chem. Phys. Letters 173 (1990) 435.
[17] Th. Weber, A.M. Smith, E. Riedle, H.J. Neusser and E.W. Schlag, Chem. Phys. Letters 175 (1990) 79.
[18] Th. Weber, E. Riedle and H.J. Neusser, Z. Physik D, in press.
[19] Th. Weber and H.J. Neusser, J. Chem. Phys., in press.
[20] E. Riedle, Th. Knittel, Th. Weber and H.J. Neusser, J. Chem. Phys. 91 (1989) 4555.
[21] T.M. Miller and B. Bederson, Advan. At. Mol. Phys. 13 (1977) 1;
S. Rauber, J.R. Klein, M.W. Cole and L.W. Bruch, Surface Sci. 123 (1982) 173.
[22] S. Leutwyler, U. Even and J. Jortner, J. Chem. Phys. 79 (1983) 5769.
[23] H.C. Longuet-Higgins and J.A. Pople, J. Chem. Phys. 27 (1957) 192.
[24] K. Yamanouchi, S. Isogai, S. Tsuchiya and K. Kuchitsu, Chem. Phys. 116 (1987) 123.
[25] T. Emilsson, T.D. Klots and H.S. Gutowsky, private communication.